Scalable Multi-Transverse-Mode Quantum Processor in Silicon Photonics

Kaveh (Hassan) Rahbardar Mojaver(1), Jelmer J. Renema(2), Odile Liboiron-Ladouceur(3)

(1) McGill University, Montréal, Canada, hassan.rahbardarmojaver@mcgill.ca
(2) MESA+ Institute, University of Twente, The Netherlands, j.j.renema@utwente.nl
(3) McGill University, Montréal, Canada, odile.liboiron-ladouceur@mcgill.ca

Abstract *We present a multi-transverse-mode quantum processor that encodes quantum states of light using the first two TE modes. The processor uses multi-mode thermo-optic phase shifters for independent mode manipulation. Using the proposed processor, we can perform a 4 x 4 optical linear transformation with only a single Mach-Zehnder interferometer. ©2023 The Author(s)*

Introduction

Over the past decades, Silicon photonics (SiPh) has garnered significant attention due to its promising attributes, including compatibility with complementary metal oxide semiconductor (CMOS), which leads to higher integration density and lower manufacturing costs [1]. Moreover, SiPh has exhibited tremendous potential in integrated quantum computing and quantum information [2]. By encoding single photons in one degree of freedom, such as polarization, path, or wavelength, optical qubits can be generated.

In recent years, path-encoded programmable quantum gates have been achieved in integrated photonics, which is a significant step towards a large-scale photonic quantum system [3]. However, encoding the information on other degrees of freedom of single photons, such as polarization and transverse mode, is crucial for the scalability of the system. Recently, there have been attempts to encode the information on orthogonal quasi-transverse modes and manipulate the information using transverse mode integrated quantum gates [4]. However, to the best of our knowledge a programmable gate/processor manipulating transverse modes has not been developed yet.

This paper proposes the Transverse Mode Encoded Programmable Quantum Processor, a novel interferometric processor that leverages the first two transverse electric (TE) modes of SiPh technology. The design continues our recent efforts on Multi-Transverse-Mode optical processors in classical computation [5]. The main advantage of the proposed transverse mode encoded programmable quantum processor is its ability to independently manipulate different transverse modes. Additionally, the processor can perform linear transformation with only one fourth of the MZIs required in a single mode path encoded counterpart. This paper will discuss the proposed processor's theoretical framework, its implementation, and its potential applications in quantum information processing.

System Level Design and Discussions

Figure 1 shows a schematic view of a 4 × 4 building block for the proposed processor. All the components used in this block have already been experimentally validated and are available in our open access multi-transverse-mode process design kit (PDK), which is compatible with standard 220 nm thick SiPh technology [6]. The key structure in this block is an MZI with two multimode input waveguides, each carrying two modes, TE0 and TE1. We use two adiabatic directional coupler-based mode multiplexer/demultiplexers (MUX/deMUX) for merging and separating the modes. The MUX converts path-encoded qubits to transverse mode-encoded qubits in a similar way that a polarization beam splitter converts polarization-encoded qubits to path-encoded ones.

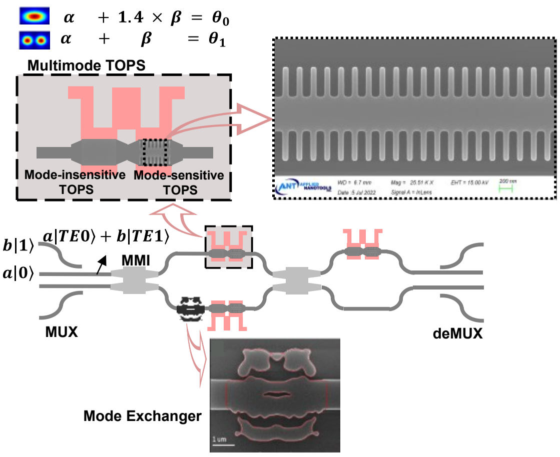

Fig. 1: A Schematic illustration of 4 × 4 building block for the Transverse Mode Encoded Programmable Quantum Processor. The block includes a multimode TOPS consisting of a mode insensitive and a mode-sensitive TOPS. It also includes a mode exchanger to convert TE0 to TE1 and vice versa.

In the input of the MUX, we have a generic path encoded qubit represented as $a|0\rangle + b|1\rangle$, where $|0\rangle$ and $|1\rangle$ are two basis states corresponding to the presence of a single photon on the first and second single mode waveguides, respectively. The single mode waveguides are 0.5 μm wide, allowing only the propagation of the fundamental TE0 mode. The MUX converts the path-encoded state to a coherent superposition of TE0 and TE1 transverse electric mode states, $a|TE0\rangle + b|TE1\rangle$, of a single photon propagating in a multi-mode waveguide where $|TE0\rangle$ and $|TE1\rangle$ are the basis states corresponding to the propagation of the single photon on TE0 and TE1 modes, respectively. The multimode waveguide is 0.96 μm wide, allowing the propagation of TE0 and TE1. We use mode insensitive MMIs from the PDK as splitters and combiners of the MZI.

The processor utilizes three multimode thermo-optic phase shifters (TOPS) - namely, δ, φ, and θ. As illustrated in Fig. 1, each multimode phase shifter comprises of two cascaded mode-insensitive and mode-sensitive phase shifters from the PDK. A mode-insensitive phase shifter is a wide waveguide with a TiW heater on top. In a previous study, we demonstrated that for a TOPS with a width greater than 4 μm, the difference between the thermo-optic coefficients for the first two TE modes is less than 2% [7]. Therefore, it applies a similar phase shift (represented as α in Fig. 1) to both TE0 and TE1.

We have recently developed a mode-sensitive TOPS using subwavelength grating (SWG) structures. These structures offers an approximately 1.4 times difference in the two thermo-optic coefficients, i.e., between the TE0 and TE1 modes. The mode-sensitive TOPS operates on the principle that TE0 propagates mainly in the 500 nm waveguide center, whereas TE1 field pattern exhibits two lobes closer to the waveguide sidewalls. The thermo-optic coefficient of silicon is an order of magnitude larger than that of oxide, i.e., 1.86×10^{-4} K^{-1} and 0.95×10^{-5} K^{-1} for silicon and SiO_2, respectively [8]. By engineering the thermo-optic coefficient of the regions closer to the waveguide sidewalls while keeping the waveguide center as silicon, we can realize large difference in the thermo-optic coefficients between TE0 and TE1. The mode-sensitive phase shifter shown in the fig. 1 applies 1.4 times larger phase shift to TE0 compared to that of TE1. For example, if the phase shift applied to TE1 is β, TE0 experiences 1.4 β of phase shift. By selecting appropriate values for α and β, we can apply any arbitrary phase shifts onto the two optical modes. For the TOPS θ, the phase shift applied to TE0 and TE1 are θ_1 and θ_2, respectively. The multimode TOPS is the key component in this design enabling independent manipulation of TE0 and TE1.

The structure also includes a mode exchanger developed using inverse design to convert TE0 to TE1 and vice versa [9]. The mode exchanger in the lower arm provides transmission between the different TE modes. Without the mode exchanger, there would be no transmission from TE0 (TE1) at the inputs to TE1 (TE0) at the outputs. By using inverse design, we achieve optimal performance and efficient footprint for the mode exchanger.

Applying the method discussed in [10], we can define the transfer matrix of the structure by multiplying the corresponding transfer matrices of the cascaded blocks from right to left:

$$\begin{bmatrix} E_{O_1-TE0} \\ E_{O_1-TE1} \\ E_{O_2-TE0} \\ E_{O_2-TE1} \end{bmatrix} = \begin{bmatrix} e^{j\phi_0} & 0 & 0 & 0 \\ 0 & e^{j\phi_1} & 0 & 0 \\ 0 & 0 & 1 & 0 \\ 0 & 0 & 0 & 1 \end{bmatrix} \times \begin{bmatrix} \sqrt{\rho} & 0 & j\sqrt{1-\rho} & 0 \\ 0 & \sqrt{\rho} & 0 & j\sqrt{1-\rho} \\ j\sqrt{1-\rho} & 0 & \sqrt{\rho} & 0 \\ 0 & j\sqrt{1-\rho} & 0 & \sqrt{\rho} \end{bmatrix} \times \begin{bmatrix} e^{j\theta_0} & 0 & 0 & 0 \\ 0 & e^{j\theta_1} & 0 & 0 \\ 0 & 0 & e^{j\delta_0} & 0 \\ 0 & 0 & 0 & e^{j\delta_1} \end{bmatrix}$$
$$\times \begin{bmatrix} 1 & 0 & 0 & 0 \\ 0 & 1 & 0 & 0 \\ 0 & 0 & 0 & 1 \\ 0 & 0 & 1 & 0 \end{bmatrix} \times \begin{bmatrix} \sqrt{\rho} & 0 & j\sqrt{1-\rho} & 0 \\ 0 & \sqrt{\rho} & 0 & j\sqrt{1-\rho} \\ j\sqrt{1-\rho} & 0 & \sqrt{\rho} & 0 \\ 0 & j\sqrt{1-\rho} & 0 & \sqrt{\rho} \end{bmatrix} \times \begin{bmatrix} E_{I_1-TE0} \\ E_{I_1-TE1} \\ E_{I_2-TE0} \\ E_{I_2-TE1} \end{bmatrix} \quad (1)$$

wherein, $E_{I_{x-TEy}}$ and $E_{O_{x-TEy}}$ are the optical field at the x^{th} input/output and y^{th} TE mode, respectively. ρ is the optical power splitting ratio of the MMIs which is equal for TE0 and TE1 due to the mode independence behavior of the MMIs. ϕ_0, θ_0 and δ_0 are the phase shifts applied to TE0 and ϕ_1, θ_1 and δ_1 are the phase shifts applied to TE1 by the TOPS ϕ, θ, and δ, respectively. For $\rho = 0.5$, the linear transformation matrix of the input optical field to the output optical field is:

$$\frac{1}{2} \times \begin{bmatrix} e^{j\phi_0+j\theta_0} & -e^{j\phi_0+j\delta_0} & je^{j\phi_0+j\theta_0} & je^{j\phi_0+j\delta_0} \\ -e^{j\phi_1+\delta_1} & e^{j\phi_1+\theta_1} & je^{j\phi_1+\delta_1} & je^{j\phi_1+\theta_1} \\ je^{j\theta_0} & je^{j\delta_0} & -e^{j\theta_0} & e^{j\delta_0} \\ je^{j\delta_1} & je^{j\theta_1} & e^{j\delta_1} & e^{j\theta_1} \end{bmatrix}$$

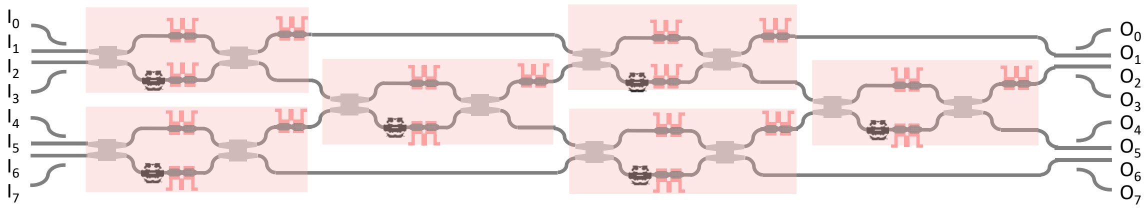

Fig. 2: A 8 × 8 Transverse Mode Encoded Programmable Quantum Processor build on a Clement mesh. This processor can perform an 8 × 8 unitary matrix transformation with only six MZIs.

By modifying the values of the three TOPS based on the presented transformation matrix, we can perform a unitary transformation on the optical fields of the two paths and two orthogonal modes. As shown in fig. 1, the presented design performs a 4 × 4 unitary transformation employing only a single MZI. In a single mode path encoding processor, a 4 × 4 unitary transformation requires a minimum of six MZIs on Reck or Clements Mesh and minimum of eight MZIs on Bokun mesh [11].

We can use the building block presented in fig.1 on a larger mesh as shown in fig. 2 to realize a linear transformation on larger dimensions. In the presented multi-transverse-mode processor, the number of MZIs required for an N × N transformation on Clements mesh is $\frac{N(N-2)}{8}$, which is asymptotically one fourth of the MZIs required in a single mode path encoded system (i.e, $\frac{N(N-1)}{2}$). The mesh depth (number of consecutive MZIs in the longest path) is also half of that of single mode path encoded system. For example, the structure shown in fig. 2 performs 8 × 8 unitary transformation with a mesh with the depth of four MZIs. A similar transformation requires a mesh depth of eight in a single-mode system.

The presented design uses multimode components such as MMIs, waveguide bends, crossings, etc., which exhibit slightly larger insertion loss compared to their single-mode structure counterparts. However, due to the 50% reduction in mesh depth, the optical insertion loss is drastically decreased, leading to overall lower optical loss and higher scalability. Furthermore, there have been recent advancements in developing SiPh multimode components for use in mode division-multiplexing (MDM) telecommunication systems [12]. We can leverage this developing trend in MDM to further decrease the insertion loss of our proposed processor and enhance its scalability.

The presented processor is capable of performing a linear transformation of quantum states. By utilizing the nondeterministic, coincidence basis method described in [13], the presented multi-transverse mode processor can be programmed to implement heralded quantum logic and entangling gates. The implementation of various gates, including heralded and non-heralded Controlled NOT (CNOT) using universal linear optics, has already been demonstrated in [14].

The proposed structure offers two main advantages compared to the transverse mode encoded Controlled NOT (CNOT) quantum gate presented in [4]. Thanks to the multimode TOPS, the presented design is programmable and can be programmed to operate as various gates, whereas [4] can only perform the CNOT operation. Moreover, our design is tunable, hence, the TOPS can be adjusted to compensate for the fabrication variations and dynamic errors generated from thermal and electrical crosstalk..

Conclusions

We proposed a multi-transverse-mode quantum processor that utilizes the first two TE modes for qubit encoding. The design offers several advantages over traditional single-mode path-encoded processors. Specifically, our multi-transverse-mode quantum processor offers 50% shorter optical depth paths and almost half the number of Mach-Zehnder interferometers required for similar transformations. By employing multi-mode thermo-optic phase shifters, we can achieve independent manipulation of optical modes, enabling programmability and compensation for fabrication variations and dynamic errors. Overall, our design provides a scalable and versatile platform for quantum information processing.

References

[1] S. Y. Siew, B. Li, F. Gao, H. Y. Zheng, W. Zhang, P. Guo, S. W. Xie, A. Song, B. Dong, L. W. Luo, C. Li, X. Luo, and G.-Q. Lo, "Review of silicon photonics technology and platform development," J. Lightw. Technol., vol. 39, no. 13, pp. 4374-4389, Jul. 2021, DOI: 10.1109/JLT.2021.3066203.

[2] X. Qiang, X. Zhou, J. Wang, C. M. Wilkes, T. Loke, S. O'Gara, L. Kling, G. D. Marshall, R. Santagati, T. C. Ralph, J. B. Wang, J. L. O'Brien, M. G. Thompson, and J. C. F. Matthews, "Large-scale silicon quantum photonics implementing arbitrary two-qubit processing," *Nature Photon*., vol. 12, pp. 534–539, Sep. 2018, DOI: 10.1038/s41566-018-0236-y

[3] C. Taballione, R. van der Meer, H. J. Snijders, P. Hooijschuur, J. P. Epping, M. de Goede, B. Kassenberg, P. Venderbosch, C. Toebes, H. van den Vlekkert, P. W. H. Pinkse, and J. J. Renema, "A universal fully reconfigurable 12-mode quantum photonic processor," Quantum Sci. Technol., vol. 1, no. 3, pp. 035002, Aug. 2021, DOI: 10.1088/2058-9565/ac168c

[4] L. Feng, M. Zhang, X. Xiong, D. Liu, Y. Cheng, F. Jing, X. Qi, Y. Chen, D. He, G. Guo, D. Dai, X. Ren, "Transverse mode-encoded quantum gate on a silicon photonic chip", *Phys. Rev. Lett.* 128, pp. 060501, Feb. 2022, DOI: 10.1103/PhysRevLett.128.060501

[5] K. R. Mojaver and O. Liboiron-Ladouceur, "On-chip Optical Phase Monitoring in Multi-Transverse-Mode Integrated Silicon-based Optical Processors," *IEEE Journal of Selected Topics in Quantum Electronics*, vol. 28, no. 6, pp. 1–7, Nov. 2022, DOI: 10.1109/JSTQE.2022.3209023.

[6] SiPh_MDM_PDK. Accessed: Apr. 24, 2023. [Online] Available: https://github.com/KavehMojaver/SiPh_MDM_PDK

[7] G. Zhang, K. R. Mojaver, A. Das, and O. Liboiron-Ladouceur, "Mode insensitive switch for on-chip interconnect mode division multiplexing systems," *Optics Letters*, vol. 45, no. 4, pp. 811–814, 2020, DOI: 10.1364/OL.384771

[8] K. R. Mojaver, G. Zhang and O. Liboiron-Ladouceur, "Design of Silicon Photonic Mode-Sensitive Thermo-Optic Phase Shifter based on Subwavelength Grating Structures," *2022 IEEE Photonics Conference (IPC)*, Vancouver, BC, Canada, pp. 1, 2, 2022, DOI: 10.1109/IPC53466.2022.9975612.

[9] G. Zhang, D.-X. Xu, Y. Grinberg, and O. Liboiron-Ladouceur, "Efficient mode exchanger-based silicon photonic switch enabled by inverse design," Opt. Express, vol. 30, no. 12, pp. 20543-20553, May 2022. DOI: 10.1364/OE.456869

[10] F. Shokraneh, S. Geoffroy-Gagnon, and O. Liboiron-Ladouceur. "High-Performance Programmable MZI-Based Optical Processors," in Silicon Photonics for High-Performance Computing and Beyond, pp. 335-365. CRC Press, 2021.

[11] K. R. Mojaver, B. Zhao, E. Leung, S. M. R. Safaee, O. Liboiron-Ladouceur, "Addressing the programming challenges of practical interferometric mesh based optical processors,". 2023, arXiv:2303.04151

[12] L. Zhang, S. Hong, Y. Wang, H. Yan, Y. Xie, T. Chen, M. Zhang, Z. Yu, Y. Shi, L. Liu, and D. Dai, "New-generation silicon photonics beyond the singlemode regime," 2021, arXiv:2104.04239

[13] T. C. Ralph, N. K. Langford, T. B. Bell, and A. G. White, "Linear optical controlled-NOT gate in the coincidence basis," PHYSICAL REVIEW A, vol. 65, p. 062324, Jun. 2002, DOI: 10.1103/PhysRevA.65.062324.

[14] J. Carolan, C. Harrold, C. Sparrow, E. Martín-López, N. J. Russell, J. W. Silverstone, P. J. Shadbolt, N. Matsuda, M. Oguma, M. Itoh, G. D. Marshall, M. G. Thompson, J. C. F. Matthews, T. Hashimoto, and J. L. O'Brien, "Universal linear optics," Science, vol. 349, no. 6249, pp. 711-716, Aug. 2015. DOI: 10.1126/science.aab3642